BIOCHEMISTRY
including biophysical chemistry & molecular biology

CURRENT TOPIC

pubs.acs.org/biochemistry

Chloride Regulation of Enzyme Turnover: Application to the Role of Chloride in Photosystem II

Ravi Pokhrel, Iain L. McConnell, and Gary W. Brudvig*

Department of Chemistry, Yale University, New Haven, Connecticut 06520-8107, United States

ABSTRACT: Chloride-dependent α-amylases, angiotensin-converting enzyme (ACE), and photosystem II (PSII) are activated by bound chloride. Chloride-binding sites in these enzymes contain a positively charged Arg or Lys residue crucial for chloride binding. In α-amylases and ACE, removal of chloride from the binding site triggers formation of a salt bridge between the positively charged Arg or Lys residue involved in chloride binding and a nearby carboxylate residue. The mechanism for chloride activation in ACE and chloride-dependent α-amylases is 2-fold: (i) correctly positioning catalytic residues or other residues involved in stabilizing the enzyme−substrate complex and (ii) fine-tuning of the pK_a of a catalytic residue. By using examples of how chloride activates α-amylases and ACE, we can gain insight into the potential mechanisms by which chloride functions in PSII. Recent structural evidence from cyanobacterial PSII indicates that there is at least one chloride-binding site in the vicinity of the oxygen-evolving complex (OEC). Here we propose that, in the absence of chloride, a salt bridge between D2:K317 and D1:D61 (and/or D1:E333) is formed. This can cause a conformational shift of D1:D61 and lower the pK_a of this residue, making it an inefficient proton acceptor during the S-state cycle. Movement of the D1:E333 ligand and the adjacent D1:H332 ligand due to chloride removal could also explain the observed change in the magnetic properties of the manganese cluster in the OEC upon chloride depletion.

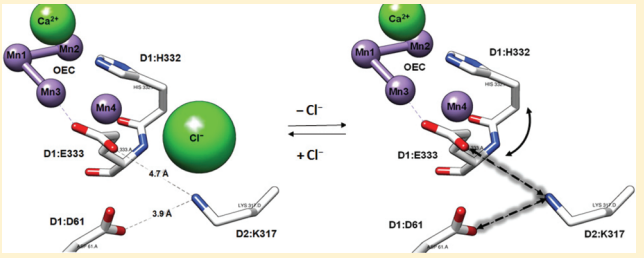

Ions are prevalent in cellular environments, and cells have well-regulated mechanisms for their transport across cell membranes. Because of their widespread availability, it is common to see ions playing a role in protein function. Metal ions are commonly involved in a variety of important functions in proteins such as protein folding and catalysis; however, use of inorganic anions, particularly Cl^-, for protein function is rare. Examples of Cl^- in biological systems include the Cl^- channel important in muscle function and signal transduction, and the bacterial chloride pump, halorhodopsin, which helps maintain the osmotic balance for halobacteria living in saturated salt solutions.[1−3] Although examples of Cl^- regulating enzyme function are scarce, photosystem II (PSII), angiotensin-converting enzyme (ACE), and some Cl^--dependent α-amylases are all activated for enzyme turnover by bound Cl^-.[4−8] The role of Cl^- as an essential cofactor for oxygen evolution in PSII has been a subject of investigation for nearly 70 years, yet the mechanism by which Cl^- activates the catalysis of water oxidation is undetermined. In this review, we discuss the role of Cl^- in Cl^--dependent α-amylases and ACE to gain insight into the mechanism by which Cl^- activates PSII. We then propose a mechanism for the function of Cl^- in PSII based upon the recent structural characterizations of the Cl^--binding sites in PSII. A detailed review with a comparison of Cl^- in PSII with other Cl^--requiring enzymes has been published by W. J. Coleman.[9] However, with new structural information about the location of Cl^- in PSII, novel mechanistic insights into the role of Cl^- in PSII can now be gained by such a comparison.

CHLORIDE IN α-AMYLASES

α-Amylase catalyzes the hydrolysis of internal α(1,4)-glycosidic bonds with net retention of the anomeric configuration in starch, amylase, amylopectin, glycogen, and other polysaccharides.[10,11] Cl^- induces an allosteric activation in some α-amylases, including the bacterial α-amylase from *Alteromonas haloplanctis*.[10,12,13] Removal of Cl^- by dialysis or gel filtration results in total inactivation of the enzyme, which is fully recovered by the addition of Cl^-, Br^-, and to a lesser extent I^- and some other monovalent anions (Table 1).[14] However, the activities of α-amylases from some other species are independent of Cl^-.

The Cl^--binding site of Cl^--dependent mammalian pancreatic and salivary α-amylases is composed of R195, N298, R337, and a water molecule (Figure 1).[15−17] These protein ligands to Cl^- are part of highly conserved regions of Cl^--dependent α-amylases.[18] In *A. haloplanctis*, the Cl^--binding site contains a lysine residue in place of R337.[14] Interestingly, the basic lysine or arginine residue is not present in Cl^--independent α-amylases. α-Amylase from *Bacillus* is a Cl^--independent α-amylase; the primary difference between the sequence of α-amylase from *Bacillus* and the sequences of Cl^--dependent α-amylases relating to the Cl^- requirement is the K/R337Q substitution in

Received: January 9, 2011
Revised: February 22, 2011
Published: March 02, 2011

Table 1. Comparison of Activating Monovalent Anions[a] That Compete for the Chloride Site in α-Amylase, ACE, and PSII[14,25,48]

Cl^--activated enzyme	competitive activators
α-amylase	$Cl^- > Br^- > NO_2^- > HCOO^- > I^- > NO_3^- > ClO_3^- > CNO^- > SCN^- > CH_3COO^- > F^- > SO_4^{2-}$
ACE	$Cl^- > Br^- > F^- > NO_3^- > CH_3COO^-$
PSII	$Cl^- > Br^- \gg NO_3^- > NO_2^- > I^-$

[a] Anions are ranked according to the efficiency with which they can replace chloride functionally.

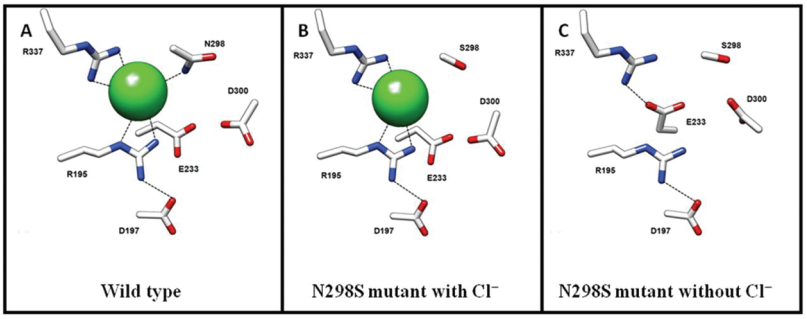

Figure 1. (A) Cl^--binding site occupied by Cl^- in wild-type human pancreatic α-amylase (HPA), (B) Cl^--binding site occupied by Cl^- in the N298S variant of HPA, and (C) vacant Cl^--binding site in the N298S variant of HPA. Panels A−C were created from Protein Data Bank entries 1HNY (1.80 Å resolution), 1XH1 (2.03 Å resolution), and 1XGZ (2.00 Å resolution), respectively.

Bacillus.[14,36] Cl^- binding experiments show that Cl^- is not bound in K337Q α-amylase from *A. haloplanctis*, and the activity of this mutant is consequently independent of Cl^-.[14]

Similarly, a series of mutants, R195A, R195Q, R337A, and R337Q, of human pancreatic α-amylase (HPA) did not show binding of Cl^-.[19] Crystal structures of these mutant enzymes showed no significant structural changes compared to the wild type.[19] However, the R195 mutations resulted in Cl^- independence, a 20−450-fold decrease in activity, and a shift of the pH optimum to a more basic pH.[19] Besides being a ligand to Cl^-, R195 is also directly hydrogen bonded to two catalytic residues in the active site, Asp197 and Glu233. The active site of α-amylases contains a catalytic triad: Asp197, Glu233, and Asp300. Asp197 acts as the catalytic nucleophile; Glu233 acts as the general acid catalyst, and Asp300 is involved in stabilizing the conformation of bound substrates.[20,21] Therefore, mutation of R195 affects aspects of catalysis, in addition to the Cl^- binding properties of the enzyme. The mutation of R337, which is located at the bottom of the Cl^--binding pocket and does not interact with the catalytic residues in the presence of Cl^-, also results in a loss of Cl^- dependence. However, because of its location, there is an only 2-fold decrease in activity in R337 mutants, and the pH profile is similar to that of wild-type HPA.[19]

For wild-type α-amylase from *A. haloplanctis*, removal of Cl^- shifts the optimal pH for activity from 7.4 to 6.2. The K_m value for wild-type α-amylase activity is independent of Cl^- concentration, but there is an ∼10-fold decrease in the k_{cat} of the enzyme upon removal of Cl^-.[14] The activity of α-amylase from *A. haloplanctis* is supported by different anions: $Cl^- > Br^- > NO_2^- > HCOO^- > I^- > NO_3^- > ClO_3^- > CNO^- > SCN^- > CH_3COO^- > F^- > SO_4^{2-}$ (Table 1).[14] All activating anions, with the exception of CH_3COO^- and F^-, induce the same shift in the optimal pH for activity in the presence and absence of an anion.[14] The Cl^--independent K337Q mutant from *A. haloplanctis* also has an optimal pH for activity of pH 7.6 regardless of the presence or absence of Cl^-. Additionally, the optimal pH for activity in the Cl^--independent α-amylase from *Bacillus*, which contains Gln in place of Lys/Arg337, is shifted to a more alkaline pH. This indicates that the catalytic mechanism is inhibited in Cl^--dependent wild-type α-amylases when the positively charged side chain (Arg/Lys337) is not neutralized by an anion,[14] suggesting that the pK_a of one or more catalytic residues is fine-tuned for maximal activity when Cl^- is shielding these residues from the electrostatic influence of the protonated Arg/Lys337 residue.

Among the catalytic residues, E233 is closest to bound Cl^- and is most likely affected by its removal (Figure 1). Several experimental arguments suggest that in Cl^--dependent α-amylases, Cl^- allows E233 to be protonated at the pH of maximal enzymatic activity.[14] The shift of pH_{opt}, pK_{app}, and the simultaneous activation upon Cl^- binding are explained by an alkaline shift in the pK_a of E233.

There is structural evidence that directly supports this observation. The N298S mutant of HPA also requires Cl^- for maximal activity. However, this mutation shifts the K_d of Cl^- from 0.52 mM in wild-type HPA to 168 mM in N298S HPA, allowing structural studies of this variant enzyme in the presence and absence of Cl^-. When the sites are occupied by Cl^-, positioning of amino acid residues in the Cl^--binding site, as well as the catalytic carboxylate residues, is similar for both wild-type and N298S HPA (see Figure 1). In N298S HPA, S298, R195, D197, and R337 maintain the same position in the absence of Cl^-, but E233 and D300 move toward the vacant Cl^- site (see Figure 1). The conformational shift of E233 is more pronounced than that of D300 because it rotates into the Cl^- site to form a salt bridge with the positively charged R337 residue (see Figure 1). Formation of a salt bridge between E233 and R337 will lower the pK_a of E233. Besides tuning the pK_a of E233, the occupancy of the Cl^- site allows for the correct positioning of the E233 and D300 residues required for high activity.

dx.doi.org/10.1021/bi2000388 |*Biochemistry* 2011, 50, 2725–2734

CHLORIDE IN THE ANGIOTENSIN-CONVERTING ENZYME

ACE, a type I membrane-anchored dipeptidyl carboxypeptidase, is essential for blood pressure regulation and electrolyte homeostasis as part of the renin−angiotensin−aldosterone system.[22] The two isoforms of ACE are transcribed from the same gene in a tissue-specific manner.[22] Germinal ACE (90−110 kDa) contains a single Zn^{2+} active site. Somatic ACE (150−180 kDa) consists of homologous N and C domains, each containing a Zn^{2+} active site,[23] with the C-terminal domain corresponding to the germinal form of ACE.[22] The N and C domains have different substrate specificities, inhibition and Cl^- activation profiles, and physiological functions.[24]

In somatic ACE, Cl^- activates hydrolysis by ACE in a substrate-dependent manner.[25,26] At pH 7.5, activity toward angiotensin I, a physiological substrate, cannot be detected without added Cl^- and reaches a maximum at 200 mM Cl^-.[25] However, bradykinin, another physiological substrate, is hydrolyzed in the absence of added Cl^-, and maximal activity is observed at 20 mM Cl^-.[25] The C domain active site in somatic ACE, corresponding to the germinal form of ACE, is highly dependent on Cl^- concentration, whereas the N domain is still active in the absence of Cl^- and is fully activated at very low Cl^- concentrations.[27]

Somatic ACE-catalyzed hydrolysis is activated by monovalent anions in the following order: $Cl^- > Br^- > F^- > NO_3^- > CH_3COO^-$ (Table 1).[25] Removal of Cl^- by extensive dialysis results in inactivation of the C and N domains, which can be reactivated by addition of Cl^- and other halides.[28] The C domain can be fully reactivated not only by Cl^- but also by F^-, Br^-, and I^- and shows an inverted bell-shaped relation between ionic size and $K_{d,app}$ for halides.[28] Cl^- and Br^- are the most tightly bound; I^- and F^- have a 10−100-fold lower affinity.[28]

Human testicular ACE (tACE) is a germinal-type ACE with a single Zn^{2+} active site and corresponds only to the C-terminal domain of the somatic ACE. tACE contains two buried chlorides separated by 20.3 Å[22] (Figure 2). The two Cl^- ions are 20.7 and 10.4 Å from the Zn^{2+} of the active site, respectively.[22] The first Cl^- ion (Cl1) is bound to four ligands (two Arg residues, a Trp, and a water) and is surrounded by a hydrophobic shell of four Trp residues.[22] The second Cl^- ion (Cl2) forms an ion pair with an Arg residue, R522.[22] R522 is crucial for the Cl^- dependence of ACE. It was shown that mutation of R1098, the analogous residue in the C domain of somatic ACE, to a glutamine led to a loss of the Cl^- dependence of activity.[28] R522 lies on the same helix as two other residues (Y520 and Y523) that interact with the substrate (Figure 3).

Tzakos et al.[29] have proposed that the removal of Cl^- triggers structural changes in the residues around the substrate-binding site (Figure 3). Without chloride, R522 forms a salt bridge with D465, causing movement of Y523 and Y520 away from the active site, where they are unable to stabilize the enzyme−substrate complex.[29] In the presence of Cl^-, the salt bridge between R522 and D465 is prevented because of ion pairing between Cl^- and R522, allowing Y523 to move toward the catalytic center and stabilize the enzyme−substrate complex.[29]

CHLORIDE IN PHOTOSYSTEM II

Photosystem II (PSII) catalyzes light-driven water oxidation in all oxygenic photosynthetic organisms. The active site of the enzyme, the oxygen-evolving complex (OEC), is an oxo-bridged

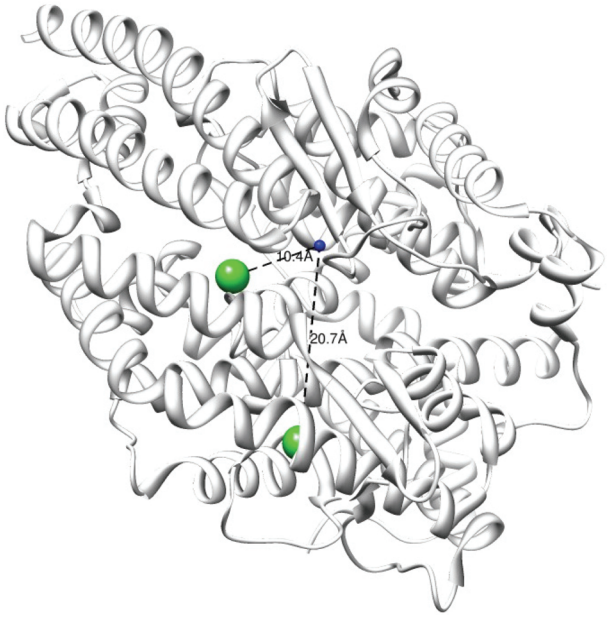

Figure 2. Location of two Cl^--binding sites (C11 and C12, green spheres) in the crystal structure of human tACE. Cl1 and Cl2 are 20.7 and 10.4 Å from the Zn^{2+} (blue sphere) in the active site, respectively (distances depicted with dashed lines). This figure was created from Protein Data Bank entry 1O86 (2.00 Å resolution).

Mn_4Ca cluster arranged in a Mn_3CaO_4 cuboidal framework with a "dangling Mn" attached via a μ-oxo group.[30] During turnover, the OEC progresses through a series of oxidation states, known as S states. The OEC is sequentially oxidized from the S_0 state, the most reduced state, to the S_4 state, the most oxidized state, using photonic energy. Transfer of photon excitation energy to the reaction center chlorophyll, P_{680}, triggers a series of electron-transfer events in PSII. In its excited state, P_{680}^* donates an electron to a membrane-bound quinone, Q_A, via a pheophytin cofactor. Because of that, a stable charge separation is formed between $P_{680}^{+\bullet}$ and $Q_A^{-\bullet}$. The OEC is oxidized by the $P_{680}^{+\bullet}$ radical via a redox-active tyrosine residue, Y_Z. Following four sequential oxidations of the OEC from the S_0 state to the S_4 state, the OEC is capable of splitting water into O_2, four protons, and four electrons. The OEC and the cofactors involved in electron transfer can be divided into the "donor side" and the "acceptor side" of PSII. The electron donor side consists of the OEC, Y_Z, and all the cofactors that reduce $P_{680}^{+\bullet}$. The electron acceptor side consists of the cofactors involved in the transfer of electrons from P_{680} to the terminal electron acceptor quinone in PSII, Q_B. A non-heme ferrous ion, whose physiological function is still unclear, lies between Q_A and Q_B. The non-heme iron has a bicarbonate ligand that can be substituted with other anions,[31−37] and thus, it may play a role in some of the anion effects observed for PSII.

It has been long known that Cl^- is essential for maximal O_2-evolving activity in PSII,[5,6,38] with a stoichiometry of approximately one high-affinity Cl^- ion per PSII determined by analyzing $^{36}Cl^-$-labeled PSII.[39] Recently, the locations of two chloride ions near the OEC have been identified by X-ray crystallography,[40−42] as discussed below. However, the role of chloride in activation of the OEC is not clear. By using the well-characterized examples of how chloride activates α-amylases and the angiotensin-converting enzyme discussed above, we can gain insight into the potential mechanisms by which chloride

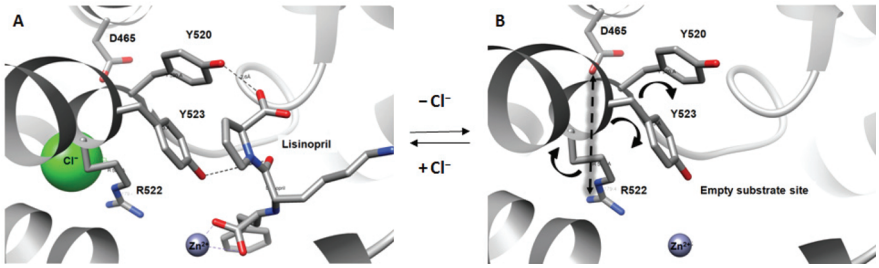

Figure 3. Mechanism proposed by Tzakos et al.[29] for activation of the C domain of ACE by Cl^- in the Cl2 site (A) and deactivation upon its removal (B), including formation of a salt bridge indicated by a dashed line and movement of residues indicated by arrows. This figure was created from Protein Data Bank entry 1O86, where lisinopril is the bound substrate in human tACE.[22]

functions in PSII. We begin with an overview of past studies of chloride in PSII and then propose a mechanism for the function of chloride in PSII that unifies these observations.

The first reports of the effects of Cl^- depletion on PSII noted that it reduced the level of steady-state turnover.[5,43] Additionally, the K_d of Cl^- varies in the presence and absence of the extrinsic subunits, PsbP and PsbQ, and depending on the Cl^- depletion procedure. In the presence of PsbP and PsbQ, Cl^- is tightly bound with a K_d of 20 μM whereas Cl^- is bound more loosely with a K_d estimate of ~1−2 mM in their absence.[44,45] When Cl^- was removed by dialysis, under conditions under which both PsbP and PsbQ remain bound, a K_d of ~500 μM was observed for Cl^- binding, which returned to a tight binding with a K_d of 20 μM when the dialyzed sample was incubated with Cl^- in darkness.[44] More recently, it has been noted that the quantum efficiency of the oxygen-evolving reaction is unchanged in Cl^--depleted PSII membranes compared to that in untreated PSII membranes.[46]

Some of the wide range of monovalent anions that compete for the Cl^--binding site in PSII are also activating, but to a lesser extent than Cl^-.[47] Oxygen-evolving activity under saturating light intensity in Cl^--depleted PSII has been recovered in the following order: $Cl^- > Br^- \gg NO_3^- > NO_2^- > I^-$ (Table 1).[48] Br^- substitutes almost identically for Cl^-. In Br^--substituted PSII, slightly lower rates of steady-state activity are reported, and the rates of substrate water exchange are decreased.[5,41,49,50] I^- is activating at low concentrations and becomes inhibitory at higher concentrations, possibly by reducing the OEC.[41,46,51,52] The activity of oxygen evolution restored by NO_3^- is almost as high as that restored by Cl^- when measured under limited light conditions.[51] Hence, NO_3^--substituted PSII is also fully active in oxygen evolution, although it has a slower turnover rate. It has been shown that NO_3^- specifically decelerates the transition from S_3 to S_0.[53] Although NO_2^- has been reported to be activating in Cl^--depleted PSII, competition of NO_2^- for the Cl^- site has not yet been studied.[48] However, there is evidence that NO_2^- inhibits PSII function.[54,55] Thermoluminescence investigations in spinach thylakoids with or without exogenous Cl^- added during the preparation indicated that NO_2^- interacts with the OEC, potentially modifying the S_2 state.[56]

Besides the activating monovalent anions, several anions and primary amines compete for the Cl^- site and are inhibitory with respect to oxygen evolution. These include the inhibitory anions F^-, N_3^-, and CH_3COO^-[57−59] and the primary amines NH_3, CH_3NH_2, $CH_3CH_2CH_2NH_2$, and $(CH_2OH)_3$-C-NH_2.[60−62] The level of competition of amines with Cl^- increases with the increasing basicity of the amine; a linear relationship is observed between the pK_a values of the amines and their apparent binding constant in thylakoid membranes.[61] A second Cl^--insensitive site is also present for ammonia binding.[60,63−65]

Flash-based UV−visible spectrophotometric measurements of PSII at 295 nm indicate that Cl^- is required for the S_2 to S_3 and S_3 to S_0 transitions, but not for the S_0 to S_1 and S_1 to S_2 transitions.[66] Even though the S_1 to S_2 transition is allowed in the absence of Cl^-, S_2/S_1 FTIR difference spectra of PSII membranes showed differences in structural changes in the S_1 to S_2 transition in the presence and absence of Cl^-.[51] Depletion of Cl^- resulted in the disappearance of a large part of the amide I and amide II vibrational modes and induced characteristic changes in the symmetric carboxylate modes. This suggests that structural changes of a carboxylate ligand to the OEC and the protein backbone are different in the presence and absence of Cl^- when the OEC advances from the S_1 state to the S_2 state. Normal spectral features were largely restored by the replenishment of Cl^-.

Location of the Cl^--Binding Site(s) in Photosystem II. Until recently, none of the published crystal structures had resolved the Cl^- ion(s); however, the location of Cl^- binding has been probed by continuous wave (CW) EPR, ESEEM, and XAS techniques. Acetate binds to PSII in the Cl^--binding site on the donor side as well as to the non-heme iron on the acceptor side.[59] CW EPR measurements of deuterated acetate-treated PSII membranes in the $S_2Y_Z^\bullet$ state suggested that acetate bound on the donor side is in the proximity (3.1 Å) of Y_Z.[67] Furthermore, ESEEM experiments with deuterated acetate-treated PSII in the $S_2Y_Z^\bullet$ state indicated that the deuterons substituted for the methyl protons of acetate could be 3−5 Å from Mn.[68] These results were interpreted as evidence that Cl^- is close to Y_Z and is a direct ligand to one of the metal ions in the OEC.

Because Br^- can functionally replace Cl^- in PSII, Br^--substituted PSII from spinach was studied by XAS at the Br K-edge to probe the Cl^--binding site of PSII in the S_1 state of the OEC.[69] Br^- absorbs at relatively high energies with weak background absorption by water, and high-quality XAS spectra can be recorded even with micromolar concentrations of PSII.[69] EXAFS analysis provided evidence that at least one metal ion, which may be Mn or Ca, is ~5 Å from Br^-.[69] This provided an argument against the popular hypothesis that Cl^- is a ligand to one of the metal ions of the OEC.

More recently, structural studies using X-ray crystallography have been conducted to identify the Cl^--binding site(s) in PSII, as shown in Figure 4. Two studies have identified two Cl^--binding sites, whereas one study identified only one of the two Cl^--binding sites.[40−42] Both sites are approximately 6−7 Å from the metal ions in the OEC and 12−15 Å from Y_Z.[40−42] One complication is that the large doses of X-rays used to obtain the

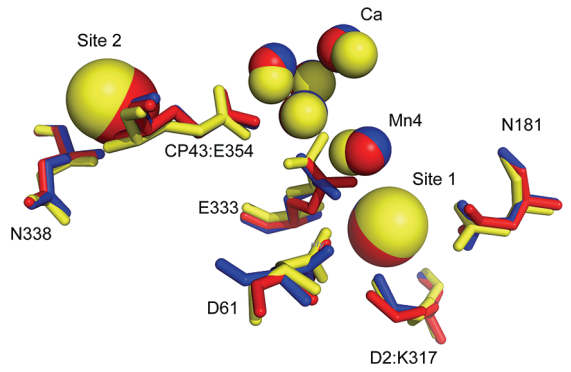

Figure 4. Cl^--binding sites from recent X-ray crystallographic structures (tentatively assigned to the S_1 state) overlaid by the align function in PyMOL as follows: yellow from Protein Data Bank entry 3A0B,[41] red from ref 40, and blue from Protein Data Bank entry 3BZ1.[42] The halides have a center-to-center distance of approximately 14 Å; site 1 is approximately 6.5 Å from Mn4, and site 2 is approximately 7 Å from Mn2. The halide at site 1 in blue is hidden by the other two that are also present there. Protein Data Bank entry 3BZ1 does not place a halide in site 2.[42] All ligands are from D1/PsbA unless otherwise labeled.

diffraction data result in chemical reduction of Mn in the OEC and cause structural changes during the X-ray diffraction measurements in the immediate vicinity of the OEC.[70] As a result, the X-ray crystal structure of the OEC obtained for the dark-stable S_1 state may be more relevant to the structure of a lower S state, such as the S_0 or S_{-1} state. Nonetheless, these studies suggest that Cl^- is not a ligand to one of the metal ions in the OEC and is rather distant from Y_Z.

Murray et al.[40] used bromide anomalous X-ray diffraction analyses to locate Cl^--binding sites in PSII isolated from the cyanobacterium *Thermosynechoccus elongatus*. Two different methods were used to obtain Br^--substituted PSII. In the first method, cells were grown in medium in which Cl^- was totally replaced with Br^-, and all buffers used for isolation of thylakoids and purified PSII core complexes contained Br^- in place of Cl^-. In the second method, cells were grown in Cl^--containing media and protein purification was conducted in the presence of Cl^-. Exchange of Br^- for Cl^- was done by incubating isolated PSII core complexes on ice for 30 min in the presence of 200 mM Br^-. X-ray data sets collected for crystals obtained from physiologically Br^--substituted PSII and Br^--infiltrated PSII were used to identify the Br^--binding sites. Anomalous X-ray diffraction of physiologically Br^--substituted PSII crystals and Br^--infiltrated PSII crystals produced consistent results indicating two Br^--binding sites in PSII. Site 1 is close to the terminal nitrogen of D2:K317 and the backbone nitrogen of D1:E333, and site 2 is in the vicinity of the backbone nitrogens of D1:N338 and CP43:E354. Both of these sites are outside the first coordination sphere of the Mn and Ca ions of the OEC and support the idea that Cl^- is not a ligand to one of the metal ions in the OEC. On the basis of the positioning of the Br^- sites (and hence the Cl^- sites) close to the postulated hydrophobic channels, the authors suggest that Cl^- facilitates the access of substrate water to and removal of protons from the OEC.

Kawakami et al.[41] also substituted Br^- and I^- for Cl^- in purified PSII cores isolated from the cyanobacterium *Thermosynechoccus vulcanus*. Anion substitution was done by incubating PSII core complexes in buffer containing 20 mM Br^- or 20 mM I^-. Diffraction data of crystals grown from Br^--substituted PSII and I^--substituted PSII had resolutions of 3.7 and 4.0 Å, respectively. Using the phase information calculated from the PSII structure without Br^- or I^- substitutions, the authors were able to calculate difference Fourier maps between the Cl^--containing PSII and Br^-- and I^--substituted PSII. Two Br^- sites and five I^- sites were identified, two of which were similar to the two Br^- sites and were, therefore, considered to be the Cl^--binding sites in PSII. These two sites agree with the Cl^--binding sites identified independently by Murray et al.[40] Because both D1:E333 and CP43:E354 bind to chloride and are also coordinated directly to metal ions in the OEC, the authors suggest that the two chloride anions are required to maintain the coordination structure of the OEC as well as the proposed proton channel to keep the OEC fully active.

Guskov et al.[42] reprocessed the X-ray diffraction data of the previously published 3.0 Å structure of PSII isolated from *T. elongatus* to a resolution of 2.9 Å. The data at 2.9 Å resolution allowed for refinement of the positions of previously assigned subunits as well as new assignments of several subunits and cofactors, including one Cl^- per PSII monomer. The electron density revealed a patch at the $\sim 4.3\sigma$ level near the OEC that was modeled and refined as a fully occupied Cl^-. In this 2.9 Å crystal structure of PSII, Cl^- is coordinated by Nε of D2:K317, Nδ of D1:N181, and the backbone N of D1:E333. In addition, *T. elongatus* cells were grown in a medium containing Br^- instead of Cl^- to isolate Br^--substituted PSII. X-ray diffraction of the Br^--substituted PSII crystals was used to compute the difference electron density at 3.9 Å resolution, and these results confirmed the Cl^--binding site identified in the 2.9 Å resolution crystal structure. The Cl^- site identified in this high-resolution structure shows only one of the Cl^- sites identified in the previously mentioned X-ray crystallographic studies of Br^--substituted PSII.

The presence of one common Cl^- site in all three structural studies indicates that the chloride ion in site 1 (D2:K317 site) is unarguably present in PSII and most likely is the high-affinity chloride site identified by $^{36}Cl^-$ labeling studies;[39] the chloride ion in site 2 (CP43:E354 site) could also be present and may be a lower-affinity site. It has been shown that some primary amines compete with Cl^- for the Cl^--binding site,[60−62] although it is unclear how amines compete for the Cl^--binding sites identified in the recent crystal structures. One possible mechanism by which amines can bind at the Cl^--binding sites is through hydrogen bonding because all the ligands to Cl^- are capable of forming hydrogen bonds with amines.

Herein, we propose a role for chloride in the function of PSII based on the structural characterization of Cl^--binding sites focusing on the role of the chloride ion in site 1 (D2:K317 site). First, however, we review studies of the effect of chloride depletion on the properties of the manganese cluster in the OEC, in view of the X-ray crystallographic evidence that chloride is associated with many of the manganese ligands.

EPR Spectroscopic Studies of Cl^--Depleted Photosystem II. Cl^--depleted PSII membranes and Cl^--depleted PSII membranes substituted with other anions have been extensively studied using EPR spectroscopy to investigate the effect of Cl^- on the S-state advancement of the OEC. The manganese cluster in the OEC predominantly gives rise to two types of EPR signals in the S_2 state, a $g = 2$ multiline signal and a $g = 4.1$ signal.[71−73] The $g = 2$ multiline signal arises from an $S = {}^1/_2$ ground state, and the broad $g = 4.1$ signal arises from the middle Kramers doublet of an $S = {}^5/_2$ state.[74,75] Amplitudes of the $g = 4.1$ signal

and the $g = 2$ multiline signal oscillate with a period of four, showing maxima on the first and fifth flashes, which is characteristic of the S_2 state.[76] Relative amounts of the $g = 4.1$ signal and the $g = 2$ multiline signal depend on the sample preparation and illumination conditions. Samples prepared in the presence of sucrose as the cryoprotectant generate both the $g = 4.1$ and $g = 2$ multiline signals upon illumination at 200 K.[77] However, the intensity of the $g = 4.1$ signal at 200 K is suppressed by the presence of glycerol, ethylene glycol, ethanol, and methanol.[76] Illumination of dark-adapted PSII at 140 K produces exclusively the $g = 4.1$ signal that can be converted to the $g = 2$ multiline signal by incubating the sample at 200 K in the dark.[72] The state responsible for the $g = 2$ multiline signal can be converted to the state responsible for the $g = 4.1$ signal upon absorption of near-IR light at ~150 K, and warming the sample to 200 K reverses the $g = 2$ to $g = 4.1$ conversion.[78]

Interestingly, illumination of dark-adapted Cl^--depleted PSII isolated from spinach at 200 K to generate the S_2 state results in the formation of the $g = 4.1$ signal in lieu of the $g = 2$ multiline signal.[79] The S_2-state multiline signal can be restored in darkness by addition of Cl^- to the illuminated sample.[80] When Cl^- is substituted with F^-, oxygen evolution is completely inhibited by preventing the S_2 to S_3 transition and the $g = 4.1$ S_2-state signal is highly enhanced over the multiline signal.[46,81] Similar results are observed when Cl^- is substituted with acetate.[82]

The decay kinetics of the population of PSII centers in the $g = 2$ multiline and $g = 4.1$ forms of the S_2 state differ markedly. The $g = 2$ multiline signal decays at 20 °C with a $t_{1/2}$ of 30 s compared to a $t_{1/2}$ of 10 min for the $g = 4.1$ signal.[80] This is in agreement with earlier results that a long-lived S_2 state was present in 40% of the centers in Cl^--depleted PSII chloroplasts.[83] Cl^--depleted PSII membranes also show an upshifted emission temperature for the $S_2Q_B^-$ charge recombination B band when probed by thermoluminescence measurements.[84] In Cl^--depleted PSII membranes substituted with F^-, the thermoluminescence B band arising from $S_2Q_B^-$ charge recombination is modified and the peak temperatures are upshifted by 13 °C.[81]

These results demonstrate that the magnetic properties of the S_2 state are affected by depletion of Cl^-, indicating that the coordination and/or magnetic interactions of the manganese ions depend on the presence or absence of Cl^-. This is consistent with the structural models from the recent X-ray crystal structures that model both D1:E333 and CP43:E354 as ligands to manganese ions and also as residues that bind Cl^- via their backbone nitrogens (Figure 4).

■ PROPOSED MECHANISM FOR ACTIVATION OF PHOTOSYSTEM II BY CHLORIDE

Cl^--binding pockets in the C domain of ACE, α-amylase, and PSII contain a positively charged Arg or Lys residue that seems to be crucial in the Cl^--binding site. Cl^- and other monovalent anions capable of competing for the Cl^- sites can form an ion pair with the positively charged residue. Reversible inactivation upon Cl^- depletion and enzyme activation by a variety of monovalent anions other than Cl^- are common aspects of these enzymes. Mutation of the positively charged Arg or Lys residue to a Gln residue in both ACE and α-amylase yields Cl^--independent enzymes, albeit with lower turnover rates.[14,28] Although PSII membranes with a D2:K317Q mutation have not yet been studied, on the basis of the other examples we would expect the activity of this mutant to be independent of Cl^-. Because of striking similarities in the halide binding and activation characteristics of these enzymes, we propose a mechanism by which Cl^- activates PSII on the basis of the results from studies of ACE and α-amylase.

In ACE, Cl^- plays a structural role in positioning the amino acid residues to stabilize the enzyme−substrate complex. In Cl^--dependent α-amylases, Cl^- tunes the pK_a of E233, the general acid catalyst, and correctly positions the catalytic residues E233 and D300; formation of a salt bridge between K337 and E233 in the absence of Cl^- reduces the pK_a of E233. We propose that the activation of PSII by Cl^- in site 1 is due to a structural change that creates an optimal structural framework of the amino acid residues around the OEC, as well as a fine-tuning of the pK_a of D1:D61, a residue proposed to be important for proton transport. In the 2.9 Å crystal structure of PSII, Cl^- is coordinated by Nε of D2:K317, Nδ of D1:N181, and the backbone N of D1:E333.[42] In the presence of Cl^-, Nε of D2:K317 is 3.9 Å from D1:D61 and 4.7 Å from D1:E333.

We propose that role of Cl^- is to break the salt bridge between protonated D2:K317 and a nearby carboxylate residue, possibly D1:D61 and/or D1:E333, that is expected to form in the absence of Cl^-. The D1:D61 residue is proposed to be involved in the transport of protons from the OEC to the lumen.[85−87] Hydrated DFT QM/MM structural models suggest an extended hydrogen bonding network from substrate water molecules via CP43:R357 to D1:D61, leading to the lumenal side of the membrane.[88] The pK_a of the D1:D61 residue must be well-tuned for the transport of protons from the OEC to the lumen. Analogous to removal of Cl^- from α-amylase, which reduces the pK_a of the Glu233 residue, a decrease in the pK_a of D1:D61 upon removal of Cl^- from PSII is expected. A downward shift in the pK_a of D1:D61 fits nicely with formation of the proposed salt bridge between D2:K317 and D1:D61 upon removal of Cl^-. A decrease in the pK_a of D1:D61 will make it an inefficient acceptor of protons from the OEC at the previous optimal pH for O_2 evolution. This would stall the release of protons from the OEC to the lumen and, therefore, stall the S-state advancement at the S_2 state because further transitions require deprotonation of the OEC.[30,89] Additionally, any conformational shift of D1:D61 during salt bridge formation could move this residue away from the OEC, preventing efficient proton transport.

Alternatively, or simultaneously, in the absence of Cl^-, protonated D2:K317 and D1:E333 could form a salt bridge. In such a scenario, the ligation of D1:E333 to the OEC[31,32,40−42,90] will be altered. Movement of the D1:E333 residue toward D2:K317 may cause movement in the D1:H332 residue as well. Because both D1:333 and D1:H332 are ligands to manganese ions in the OEC, a structural perturbation of these residues could affect the exchange interactions of the manganese ions in the OEC and result in altered magnetic properties of the manganese cluster.

We hypothesize that an electrostatic attraction between D1:E333 and D2:K317 in the absence of Cl^- may cause changes in the coordination of the manganese ions in the OEC. Slight changes in coordination of the manganese ions in the OEC in the presence and absence of Cl^- could change the interactions between the manganese ions in the cluster, thereby changing the ground spin state. This is consistent with the experimental observation that illumination of dark-adapted Cl^--depleted PSII isolated from spinach produces the S_2-state $g = 4.1$ signal at the expense of the multiline signal.[79] The proposal of formation of a salt bridge between the protonated D2:K317 residue and the manganese-coordinating D1:E333 residue upon removal of Cl^-

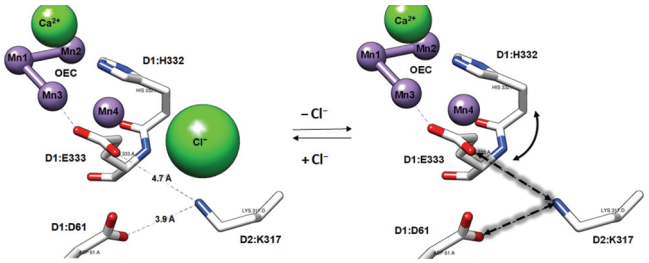

Figure 5. Proposed mechanism for the role of Cl^- in PSII function. Cl^- in site 1 is proposed to have a structural role in maintaining the optimal structural framework of the ligands to the metal ions in the OEC, as well as a role in tuning the pK_a and positioning of the D1:D61 residue proposed to be important for proton transport. Upon removal of Cl^-, D1:D61 and D1:E333 will tend to move closer to the protonated D2:K317 for a favorable electrostatic interaction. This will lower the pK_a of D1:D61 and make it an inefficient proton acceptor. Movement of D1:E333 and neighboring D1:H332 (ligands to manganese ions in the OEC) could account for the change in the ground spin state of the OEC upon removal of Cl^-.

in the D2:K317 site is, thus, consistent with the observation of a change in the ground spin state of the tetranuclear manganese cluster.

In the S_2 state, the oxidation states of the manganese ions in the OEC are assigned to be Mn_4(III,IV,IV,IV).[91−95] EXAFS experiments have shown that the OEC in the S_2 state contains 2−3 2.7 Å Mn−Mn distances and one 3.3 Å Mn−Mn distance.[96−98] On the basis of studies of manganese model complexes, we expect that isotropic exchange interactions between di-μ-oxo-bridged Mn ions that are 2.7−2.85 Å apart will result in a strong antiferromagnetic exchange coupling ($J < -100$ cm^{-1}),[99−102] whereas the longer 3.3 Å mono-μ-oxo-bridged Mn ions can exhibit either antiferromagnetic or ferromagnetic exchange coupling (-40 cm^{-1} $< J <$ 20 cm^{-1}).[102] Furthermore, EXAFS experiments indicate that the structures of the OEC giving rise to the $g = 4.1$ signal and the $g = 2$ multiline signal are very similar, with the only observed change being the lengthening of one of the 2.7 Å Mn−Mn distances to 2.85 Å.[103] Using experimental results from CW EPR and ^{55}Mn ENDOR spectroscopy of the S_2-state multiline signal, Peloquin et al.[104] have shown that a trimer−monomer structural model of the tetranuclear cluster best fits the spectroscopic data. In their study, a strongly antiferromagnetically coupled trimer along with a weak antiferromagnetic coupling between the monomer and the trimer resulted in an $S = {}^1/_2$ ground spin state. However, a switch from the weak antiferromagnetic exchange coupling between the monomer and the trimer to a ferromagnetic exchange coupling could change the ground spin state to an $S = {}^5/_2$ state;[93,104] switching the exchange coupling between the monomer and the trimer from weakly antiferromagnetic to ferromagnetic coupling could also result in an $S = {}^7/_2$ ground spin state.[93] Such a switch in the exchange coupling could occur as a result of a slight change in the bond angle of a mono-μ-oxo bridge between the trimer core and the monomer.[93] Alternatively, a change in the exchange coupling scheme of the OEC could be the result of a change in the location of Mn(III) in the S_2 state of the tetranuclear manganese cluster. The valence arrangement that gives rise to the S_2-state $g = 2$ multiline signal has Mn(III) on either end of the trimer core.[93] However, an $S = {}^5/_2$ ground spin state is possible if there is a change in the sign of the exchange coupling between the monomer and trimer and if Mn(III) resides at the center of the trimer core.[93]

Valence isomerization due to differences in ligation and a change in the sign of exchange coupling through a single μ-oxo bridge between manganese ions as a result of differences in ligation both have precedence. DFT-QM/MM models of the OEC have shown that two valence isomers are possible in the S_1 state, where the oxidation state of the tetranuclear manganese cluster is Mn_4(III,III,IV,IV).[88] The isomerization depends on the coordination number of the "dangler Mn", Mn4, and Mn2 (see Figure 5 for numbering), with an oxidation state of IV favored when there are six ligands to Mn and an oxidation state of III with five ligands. In the computationally modeled redox isomers, Mn2 and Mn4 have different ligation patterns. For one model, a strained conformation of the His332 ligand to Mn2 yields weak binding of this ligand, stabilizing the oxidation state of III for Mn2 with a Jahn−Teller elongation along the Mn−His332 axis and, consequently, an oxidation state of IV for Mn4 with six ligands. In the other redox isomer, better binding of the His332 ligand favors an oxidation state of IV for Mn2, and a pentacoordinated Mn4 favors an oxidation state of III for Mn4. This clearly demonstrates that a change in the ligation scheme of the Mn ions in the OEC could also lead to valence isomerization in the S_2 state. In this regard, studies of inorganic manganese complexes have shown that an exchange coupling through a mono-μ-oxo bridge between two manganese ions can vary from antiferromagnetic ($J < 0$) to weakly ferromagnetic ($J > 0$) depending on the terminal ligands.[105,106]

In the S_2 state in the presence of Cl^-, E333 is most likely a bridging ligand between Mn3 and Mn4 and His332 is a ligand to Mn2. An antiferromagnetic coupling between Mn4 and the core allows for an $S = {}^1/_2$ ground spin state giving rise to the S_2-state $g = 2$ multiline EPR signal. Movement of these residues in the absence of Cl^- could switch the exchange coupling between the dangling manganese and the core and/or trigger a valence isomerization within the manganese cluster, thereby changing the ground spin state from an $S = {}^1/_2$ state to an $S = {}^5/_2$ state and changing the populations of the S_2-state multiline and $g = 4.1$ signals.

CONCLUSION

Similarities in the ligand composition of the Cl^--binding sites along with similarities in the halide binding and activation characteristics in Cl^--dependent α-amylases, ACE, and PSII inspired us to look carefully at the mechanism by which Cl^- is activating in these enzymes. By analyzing the mechanisms by which Cl^- is activating in Cl^--dependent α-amylases and ACE, we can propose a mechanism by which Cl^- is activating in PSII. We propose that in the absence of Cl^-, a salt bridge between D2:K317 and D1:D61 (and/or D1:E333) is formed. This can cause a conformational shift of D1:D61 and lower its pK_a, making it an inefficient proton acceptor during the S-state cycle. Movement of the D1:E333 ligand and the adjacent D1:H332 ligand due to the removal of Cl^- could also account for the observed change in the magnetic properties of the manganese cluster in the OEC upon depletion of Cl^-. This proposal unifies the latest structural revelations of the Cl^--binding sites in PSII with the available biochemical and spectroscopic data for the Cl^- activation of PSII.

AUTHOR INFORMATION

Corresponding Author

*E-mail: gary.brudvig@yale.edu. Phone: (203) 432-5202. Fax: (203) 432-6144.

■ ABBREVIATIONS

ACE, angiotensin-converting enzyme; D1, D1 polypeptide of PSII; D2, D2 polypeptide of PSII; EPR, electron paramagnetic resonance; ENDOR, electron nuclear double resonance; ESEEM, electron spin echo envelope modulation; EXAFS, extended X-ray absorption fine structure; HPA, human pancreatic α-amylase; OEC, oxygen-evolving complex; PSII, photosystem II; XAS, X-ray absorption spectroscopy.

■ REFERENCES

(1) Jentsch, T. J., Stein, V., Weinreich, F., and Zdebik, A. A. (2002) Molecular structure and physiological function of chloride channels. *Physiol. Rev. 82*, 503–568.

(2) Schobert, B., and Lanyi, J. K. (1982) Halorhodopsin is a light-driven chloride pump. *J. Biol. Chem. 257*, 10306–10313.

(3) Oesterhelt, D. (1995) Structure and function of halorhodopsin. *Isr. J. Chem. 35*, 475–494.

(4) Lifshitz, R., and Levitzki, A. (1976) Identity and properties of the chloride effector binding site in hog pancreatic α-amylase. *Biochemistry 15*, 1987–1993.

(5) Warburg, O., and Lüttgens, W. (1944) Weitere experimente zur kohlensäureassimilation. *Naturwissenschaften 32*, 301.

(6) Arnon, D. I., and Whatley, F. R. (1949) Is chloride a coenzyme of photosynthesis? *Science 110*, 554–556.

(7) Skeggs, L. T., Marsh, W. H., Kahn, J. R., and Shumway, N. P. (1954) Existence of two forms of hypertensin. *J. Exp. Med. 99*, 275–282.

(8) Levitzki, A., and Steer, M. L. (1974) Allosteric activation of mammalian α-amylase by chloride. *Eur. J. Biochem. 41*, 171–180.

(9) Coleman, W. J. (1990) Chloride binding-proteins: Mechanistic implications for the oxygen-evolving complex of photosystem II. *Photosynth. Res. 23*, 1–27.

(10) Thoma, J. A., Spradlin, J. E., and Dygert, S. (1971) Plant and animal amylases. *Enzymes*, 3rd ed., Vol. 5, pp 115−189, Academic Press, San Diego.

(11) Zechel, D. L., and Withers, S. G. (2000) Glycosidase mechanisms: Anatomy of a finely tuned catalyst. *Acc. Chem. Res. 33*, 11–18.

(12) Feller, G., Lonhienne, T., Deroanne, C., Libioulle, C., Van Beeumen, J., and Gerday, C. (1992) Purification, characterization, and nucleotide sequence of the thermolabile α-amylase from the Antarctic psychrotroph *Alteromonas haloplanctis* A23. *J. Biol. Chem. 267*, 5217–5221.

(13) Feller, G., Payan, F., Theys, F., Qian, M., Haser, R., and Gerday, C. (1994) Stability and structural analysis of α-amylase from the Antarctic psychrophile *Alteromonas haloplanctis* A23. *Eur. J. Biochem. 222*, 441–447.

(14) Feller, G., le Bussy, O., Houssier, C., and Gerday, C. (1996) Structural and functional aspects of chloride binding to *Alteromonas haloplanctis* α-amylase. *J. Biol. Chem. 271*, 23836–23841.

(15) Brayer, G. D., Luo, Y., and Withers, S. G. (1995) The structure of human pancreatic α-amylase at 1.8 Å resolution and comparisons with related enzymes. *Protein Sci. 4*, 1730–1742.

(16) Qian, M., Haser, R., and Payan, F. (1993) Structure and molecular model refinement of pig pancreatic α-amylase at 2.1 Å resolution. *J. Mol. Biol. 231*, 785–799.

(17) Larson, S. B., Greenwood, A., Cascio, D., Day, J., and McPherson, A. (1994) Refined molecular structure of pig pancreatic α-amylase at 2.1 Å resolution. *J. Mol. Biol. 235*, 1560–1584.

(18) Janecek, S. (1994) Sequence similarities and evolutionary relationships of microbial, plant and animal α-amylases. *Eur. J. Biochem. 224*, 519–524.

(19) Numao, S., Maurus, R., Sidhu, G., Wang, Y., Overall, C. M., Brayer, G. D., and Withers, S. G. (2002) Probing the role of the chloride ion in the mechanism of human pancreatic α-amylase. *Biochemistry 41*, 215–225.

(20) Uitdehaag, J. C. M., Mosi, R., Kalk, K. H., Van Der Veen, B. A., Dijkhuizen, L., Withers, S. G., and Dijkstra, B. W. (1999) X-ray structures along the reaction pathway of cyclodextrin glycosyltransferase elucidate catalysis in the α-amylase family. *Nat. Struct. Biol. 6*, 432–436.

(21) Rydberg, E. H., Li, C., Maurus, R., Overall, C. M., Brayer, G. D., and Withers, S. G. (2002) Mechanistic analyses of catalysis in human pancreatic α-amylase: Detailed kinetic and structural studies of mutants of three conserved carboxylic acids. *Biochemistry 41*, 4492–4502.

(22) Natesh, R., Schwager, S. L. U., Sturrock, E. D., and Acharya, K. R. (2003) Crystal structure of the human angiotensin-converting enzyme−lisinopril complex. *Nature 421*, 551–554.

(23) Soubrier, F., Alhenc-Gelas, F., Hubert, C., Allegrini, J., John, M., Tregear, G., and Corvol, P. (1988) Two putative active centers in human angiotensin I-converting enzyme revealed by molecular cloning. *Proc. Natl. Acad. Sci. U.S.A. 85*, 9386–9390.

(24) Wei, L., Clauser, E., Alhenc-Gelas, F., and Corvol, P. (1992) The two homologous domains of human angiotensin I-converting enzyme interact differently with competitive inhibitors. *J. Biol. Chem. 267*, 13398–13405.

(25) Buenning, P., and Riordan, J. F. (1983) Activation of angiotensin converting enzyme by monovalent anions. *Biochemistry 22*, 110–116.

(26) Shapiro, R., Holmquist, B., and Riordan, J. F. (1983) Anion activation of angiotensin converting enzyme: Dependence on nature of substrate. *Biochemistry 22*, 3850–3857.

(27) Jaspard, E., Wei, L., and Alhenc-Gelas, F. (1993) Differences in the properties and enzymatic specificities of the two active sites of angiotensin I-converting enzyme (kininase II). Studies with bradykinin and other natural peptides. *J. Biol. Chem. 268*, 9496–9503.

(28) Liu, X., Fernandez, M., Wouters, M., Heyberger, S., and Husain, A. (2001) Arg1098 is critical for the chloride dependence of human angiotensin I-converting enzyme C-domain catalytic activity. *J. Biol. Chem. 276*, 33518–33525.

(29) Tzakos, A. G., Galanis, A. S., Spyroulias, G. A., Cordopatis, P., Manessi-Zoupa, E., and Gerothanassis, I. P. (2003) Structure-function discrimination of the N- and C-catalytic domains of human angiotensin-converting enzyme: Implications for Cl^- activation and peptide hydrolysis mechanisms. *Protein Eng. 16*, 993–1003.

(30) McEvoy, J. P., and Brudvig, G. W. (2006) Water splitting chemistry of photosystem II. *Chem. Rev. 106*, 4455–4483.

(31) Ferreira, K. N., Iverson, T. M., Maghlaoui, K., Barber, J., and Iwata, S. (2004) Architecture of the photosynthetic oxygen-evolving center. *Science 303*, 1831–1838.

(32) Loll, B., Kern, J., Saenger, W., Zouni, A., and Biesiadka, J. (2005) Towards complete cofactor arrangement in the 3.0 Å resolution structure of photosystem II. *Nature 438*, 1040–1044.

(33) Diner, B. A., and Petrouleas, V. (1990) Formation by nitric oxide of nitrosyl adducts of redox components of the photosystem II reaction center. II. Evidence that bicarbonate/carbon dioxide binds to the acceptor-side non-heme iron. *Biochim. Biophys. Acta 1015*, 141–149.

(34) Hienerwadel, R., and Berthomieu, C. (1995) Bicarbonate binding to the non-heme iron of photosystem II, investigated by Fourier transform infrared difference spectroscopy and ^{13}C-labeled bicarbonate. *Biochemistry 34*, 16288–16297.

(35) Petrouleas, V., Deligiannakis, Y., and Diner, B. A. (1994) Binding of carboxylate anions at the non-heme Fe(II) of PSII. II. Competition with bicarbonate and effects on the Q_A/Q_B electron transfer rate. *Biochim. Biophys. Acta 1188*, 271–277.

(36) Deligiannakis, Y., Petrouleas, V., and Diner, B. A. (1994) Binding of carboxylate anions at the non-heme Fe(II) of PS II. I. Effects on the Q_AFe^{2+} and Q_AFe^{3+} EPR spectra and the redox properties of the iron. *Biochim. Biophys. Acta 1188*, 260–270.

(37) Eaton-Rye, J. J., Blubaugh, D. J., and Govindjee (1986) Action of bicarbonate on photosynthetic electron transport in the presence or absence of inhibitory anions. *Ion Interact. Energy Transfer Biomembr., [Proc. Int. Workshop]*, 263–278.

(38) Critchley, C. (1985) The role of chloride in photosystem II. *Biochim. Biophys. Acta 811*, 33–46.

(39) Lindberg, K., Vänngård, T., and Andréasson, L. E. (1993) Studies of the slowly exchanging chloride in photosystem II of higher plants. *Photosynth. Res. 38*, 401–408.

(40) Murray, J. W., Maghlaoui, K., Joanna, K., Naoko, I., Lai, T.-L., Rutherford, A. W., Sugiura, M., Boussac, A., and Barber, J. (2008) X-ray crystallography identifies two chloride binding sites in the oxygen-evolving centre of photosystem II. *Energ. Environ. Sci. 1*, 161–166.

(41) Kawakami, K., Umena, Y., Kamiya, N., and Shen, J. R. (2009) Location of chloride and its possible functions in oxygen-evolving photosystem II revealed by X-ray crystallography. *Proc. Natl. Acad. Sci. U.S.A. 106*, 8567–8572.

(42) Guskov, A., Kern, J., Gabdulkhakov, A., Broser, M., Zouni, A., and Saenger, W. (2009) Cyanobacterial photosystem II at 2.9 Å resolution and the role of quinones, lipids, channels and chloride. *Nat. Struct. Mol. Biol. 16*, 334–342.

(43) Izawa, S., Heath, R. L., and Hind, G. (1969) The role of Cl^- in photosynthesis. The effect of artificial e^- donors upon electron transport. *Biochim. Biophys. Acta 180*, 388–398.

(44) Lindberg, K., and Andréasson, L. E. (1996) A one-site, two-state model for the binding of anions in photosystem II. *Biochemistry 35*, 14259–14267.

(45) Homann, P. H. (1988) Chloride relations of photosystem II membrane preparations depleted of, and resupplied with, their 17 kDa and 23 kDa extrinsic polypeptides. *Photosynth. Res. 15*, 205–220.

(46) Olesen, K., and Andréasson, L. E. (2003) The function of the chloride ion in photosynthetic oxygen evolution. *Biochemistry 42*, 2025–2035.

(47) Popelková, H., and Yocum, C. F. (2007) Current status of the role of Cl^- ion in the oxygen-evolving complex. *Photosynth. Res. 93*, 111–121.

(48) Wincencjusz, H., Yocum, C. F., and van Gorkom, H. J. (1999) Activating anions that replace Cl^- in the O_2-evolving complex of photosystem II slow the kinetics of the terminal step in water oxidation and destabilize the S_2 and S_3 states. *Biochemistry 38*, 3719–3725.

(49) Ishida, N., Sugiura, M., Rappaport, F., Lai, T. L., Rutherford, A. W., and Boussac, A. (2008) Biosynthetic exchange of bromide for chloride and strontium for calcium in the photosystem II oxygen-evolving enzymes. *J. Biol. Chem. 283*, 13330–13340.

(50) Beckmann, K., Ishida, N., Boussac, A., and Messinger, J. (2007) Effects of the calcium/strontium and chloride/bromide substitution on substrate water exchange rates in photosystem II. *Photosynth. Res. 91*, 176–176.

(51) Hasegawa, K., Kimura, Y., and Ono, T. A. (2002) Chloride cofactor in the photosynthetic oxygen-evolving complex studied by fourier transform infrared spectroscopy. *Biochemistry 41*, 13839–13850.

(52) Bryson, D. I., Doctor, N., Johnson, R., Baranov, S., and Haddy, A. (2005) Characteristics of iodide activation and inhibition of oxygen evolution by photosystem II. *Biochemistry 44*, 7354–7360.

(53) Wincencjusz, H., Yocum, C. F., and van Gorkom, H. J. (1998) S-state dependence of chloride binding affinities and exchange dynamics in the intact and polypeptide-depleted O_2-evolving complex of photosystem II. *Biochemistry 37*, 8595–8604.

(54) Spiller, H., and Boger, P. (1971) Photosynthetic nitrite reduction by dithioerytritol and the effect of nitrite on electron transport in isolated chloroplasts. *Photochem. Photobiol. 26*, 397–402.

(55) Stemler, A. J., and Murphy, J. B. (1985) Bicarbonate-reversible and irreversible inhibition of PS II by monovalent anions. *Plant Physiol. 77*, 974–977.

(56) Sahay, A., Jajoo, A., and Bharti, S. (2006) A thermoluminescence study of the effects of nitrite on photosystem II in spinach thylakoids. *Luminescence 21*, 143–147.

(57) Kuntzleman, T., and Haddy, A. (2009) Fluoride inhibition of photosystem II and the effect of the removal of the PsbQ subunit. *Photosynth. Res. 102*, 7–19.

(58) Haddy, A., Hatchell, J. A., Kimel, R. A., and Thomas, R. (1999) Azide as a competitor of chloride in oxygen evolution by photosystem II. *Biochemistry 38*, 6104–6110.

(59) Kühne, H., Szalai, V. A., and Brudvig, G. W. (1999) Competitive binding of acetate and chloride in photosystem II. *Biochemistry 38*, 6604–6613.

(60) Sandusky, P. O., and Yocum, C. F. (1984) The chloride requirement for photosynthetic oxygen evolution: Analysis of the effects of chloride and other anions on amine inhibition of the oxygen-evolving complex. *Biochim. Biophys. Acta 766*, 603–611.

(61) Sandusky, P. O., and Yocum, C. F. (1986) The chloride requirement for photosynthetic oxygen evolution: Factors affecting nucleophilic displacement of chloride from the oxygen-evolving complex. *Biochim. Biophys. Acta 849*, 85–93.

(62) Homann, P. H. (1988) The chloride and calcium requirement of photosynthetic water oxidation: Effects of pH. *Biochim. Biophys. Acta 934*, 1–13.

(63) Beck, W. F., de Paula, J. C., and Brudvig, G. W. (1986) Ammonia binds to the manganese site of the O_2-evolving complex of photosystem II in the S_2 state. *J. Am. Chem. Soc. 108*, 4018–4022.

(64) Beck, W. F., and Brudvig, G. W. (1986) Binding of amines to the O_2-evolving center of photosystem II. *Biochemistry 25*, 6479–6486.

(65) Beck, W. F., and Brudvig, G. W. (1988) Ligand-substitution reactions of the molecular oxygen-evolving center of photosystem II. *Chem. Scr. 28A*, 93–98.

(66) Wincencjusz, H., van Gorkom, H. J., and Yocum, C. F. (1997) The photosynthetic oxygen-evolving complex requires chloride for its redox state $S_2 \rightarrow S_3$ and $S_3 \rightarrow S_0$ transitions but not for $S_0 \rightarrow S_1$ or $S_1 \rightarrow S_2$ transitions. *Biochemistry 36*, 3663–3670.

(67) Force, D. A., Randall, D. W., and Britt, R. D. (1997) Proximity of acetate, manganese, and exchangeable deuterons to tyrosine $Y_Z^\bullet$ in acetate-inhibited photosystem II membranes: Implications for the direct involvement of $Y_Z^\bullet$ in water-splitting. *Biochemistry 36*, 12062–12070.

(68) Clemens, K. L., Force, D. A., and Britt, R. D. (2002) Acetate binding at the photosystem II oxygen-evolving complex: An S_2-state multiline mignal ESEEM study. *J. Am. Chem. Soc. 124*, 10921–10933.

(69) Haumann, M., Barra, M., Loja, P., Loscher, S., Krivanek, R., Grundmeier, A., Andréasson, L. E., and Dau, H. (2006) Bromide does not bind to the Mn_4Ca complex in its S_1 state in Cl^--depleted and Br^--reconstituted oxygen-evolving photosystem II: Evidence from X-ray absorption spectroscopy at the Br K-edge. *Biochemistry 45*, 13101–13107.

(70) Yano, J., Kern, J., Irrgang, K. D., Latimer, M. J., Bergmann, U., Glatzel, P., Pushkar, Y., Biesiadka, J., Loll, B., Sauer, K., Messinger, J., Zouni, A., and Yachandra, V. K. (2005) X-ray damage to the Mn_4Ca complex in single crystals of photosystem II: A case study for metalloprotein crystallography. *Proc. Natl. Acad. Sci. U.S.A. 102*, 12047–12052.

(71) Dismukes, G. C., and Siderer, Y. (1981) Intermediates of a polynuclear manganese center involved in photosynthetic oxidation of water. *Proc. Natl. Acad. Sci. U.S.A. 78*, 274–278.

(72) Casey, J. L., and Sauer, K. (1984) EPR detection of a cryogenically photogenerated intermediate in photosynthetic oxygen evolution. *Biochim. Biophys. Acta 767*, 21–28.

(73) Miller, A. F., and Brudvig, G. W. (1991) A guide to electron paramagnetic resonance spectroscopy of photosystem II membranes. *Biochim. Biophys. Acta 1056*, 1–18.

(74) Haddy, A., Dunham, W. R., Sands, R. H., and Aasa, R. (1992) Multifrequency EPR investigations into the origin of the S_2-state signal at $g = 4$ of the O_2-evolving complex. *Biochim. Biophys. Acta 1099*, 25–34.

(75) Haddy, A., Lakshmi, K. V., Brudvig, G. W., and Frank, H. A. (2004) Q-band EPR of the S_2 state of photosystem II confirms an S=5/2 origin of the X-band $g = 4.1$ Signal. *Biophys. J. 87*, 2885–2896.

(76) Zimmermann, J. L., and Rutherford, A. W. (1986) Electron paramagnetic resonance properties of the S_2 state of the oxygen-evolving complex of photosystem II. *Biochemistry 25*, 4609–4615.

(77) de Paula, J. C., Beck, W. F., Miller, A.-F., Wilson, R. B., and Brudvig, G. W. (1987) Studies of the manganese site of photosystem II by electron spin resonance spectroscopy. *J. Chem. Soc., Faraday Trans. 83*, 3635–3651.

(78) Boussac, A., Girerd, J. J., and Rutherford, A. W. (1996) Conversion of the spin state of the manganese complex in photosystem II induced by near-infrared light. *Biochemistry 35*, 6984–6989.

(79) Van Vliet, P., and Rutherford, A. W. (1996) Properties of the chloride-depleted oxygen-evolving complex of photosystem II studied by electron paramagnetic resonance. *Biochemistry 35*, 1829–1839.

(80) Ono, T., Zimmerman, J. L., Inoue, Y., and Rutherford, A. W. (1986) EPR evidence for a modified S-state transition in chloride-depleted photosystem II. *Biochim. Biophys. Acta 851*, 193–201.

(81) Ono, T., Nakayama, H., Gleiter, H., Inoue, Y., and Kawamori, A. (1987) Modification of the properties of S_2 state in photosynthetic oxygen-evolving center by replacement of chloride with other anions. *Arch. Biochem. Biophys. 256*, 618–624.

(82) Szalai, V. A., and Brudvig, G. W. (1996) Formation and decay of the S_3 EPR signal species in acetate-inhibited photosystem II. *Biochemistry 35*, 1946–1953.

(83) Muallem, A., Farineau, J., Laine-Boszormenyi, M., and Izawa, S. (1981) Charge storage in chloride ion depleted chloroplasts. *Photosynth., Proc. Int. Congr. 2*, 435–443.

(84) Homann, P. H., Gleiter, H., Ono, T., and Inoue, Y. (1986) Storage of abnormal oxidants Σ1, Σ2 and Σ3 in photosynthetic water oxidases inhibited by Cl^- removal. *Biochim. Biophys. Acta 850*, 10–20.

(85) Ishikita, H., Saenger, W., Loll, B., Biesiadka, J., and Knapp, E.-W. (2006) Energetics of a possible proton exit pathway for water oxidation in photosystem II. *Biochemistry 45*, 2063–2071.

(86) Sproviero, E. M., Gascón, J. A., McEvoy, J. P., Brudvig, G., and Batista, E. R. (2006) QM/MM models of the O_2-evolving complex of photosystem II. *J. Chem. Theory Comput. 2*, 1119–1134.

(87) Singh, S., Debus, R. J., Wydrzynski, T., and Hillier, W. (2008) Investigation of substrate water interactions at the high-affinity Mn site in the photosystem II oxygen-evolving complex. *Philos. Trans. R. Soc. London, Ser. B 363*, 1229–1234.

(88) Sproviero, E. M., Gascon, J. A., McEvoy, J. P., Brudvig, G. W., and Batista, V. S. (2008) Computational studies of the O_2-evolving complex of photosystem II and biomimetic oxomanganese complexes. *Coord. Chem. Rev. 252*, 395–415.

(89) Dau, H., and Haumann, M. (2008) Eight steps preceding O-O bond formation in oxygenic photosynthesis: A basic reaction cycle of the photosystem II manganese complex. *Biochim. Biophys. Acta 1767*, 472–483.

(90) Yano, J., Kern, J., Sauer, K., Latimer, M. J., Pushkar, Y., Biesiadka, J., Loll, B., Saenger, W., Messinger, J., Zouni, A., and Yachandra, V. K. (2006) Where water is oxidized to dioxygen: Structure of the photosynthetic Mn_4Ca cluster. *Science 314*, 821–825.

(91) Kulik, L. V., Epel, B., Lubitz, W., and Messinger, J. (2005) ^{55}Mn pulse ENDOR at 34 GHz of the S_0 and S_2 states of the oxygen-evolving complex in photosystem II. *J. Am. Chem. Soc. 127*, 2392–2393.

(92) Haumann, M., Mueller, C., Liebisch, P., Iuzzolino, L., Dittmer, J., Grabolle, M., Neisius, T., Meyer-Klaucke, W., and Dau, H. (2005) Structural and oxidation state changes of the photosystem II manganese complex in four transitions of the water oxidation cycle ($S_0 \rightarrow S_1$, $S_1 \rightarrow S_2$, $S_2 \rightarrow S_3$, and $S_{3,4} \rightarrow S_0$) characterized by X-ray absorption spectroscopy at 20 K and room temperature. *Biochemistry 44*, 1894–1908.

(93) Peloquin, J. M., and Britt, R. D. (2001) EPR/ENDOR characterization of the physical and electronic structure of the OEC Mn cluster. *Biochim. Biophys. Acta 1503*, 96–111.

(94) Campbell, K. A., Peloquin, J. M., Pham, D. P., Debus, R. J., and Britt, R. D. (1998) Parallel polarization EPR detection of an S_1-state "multiline" EPR signal in photosystem II particles from *Synechocystis* sp. PCC 6803. *J. Am. Chem. Soc. 120*, 447–448.

(95) Dau, H., Iuzzolino, L., and Dittmer, J. (2001) The tetramanganese complex of photosystem II during its redox cycle: X-ray absorption results and mechanistic implications. *Biochim. Biophys. Acta 1503*, 24–39.

(96) Iuzzolino, L., Dittmer, J., Doerner, W., Meyer-Klaucke, W., and Dau, H. (1998) X-ray absorption spectroscopy on layered photosystem II membrane particles suggests manganese-centered oxidation of the oxygen-evolving complex for the S_0-S_1, S_1-S_2, and S_2-S_3 transitions of the water oxidation cycle. *Biochemistry 37*, 17112–17119.

(97) Schiller, H., Dittmer, J., Iuzzolino, L., Doerner, W., Meyer-Klaucke, W., Sole, V. A., Nolting, H. F., and Dau, H. (1998) Structure and orientation of the oxygen-evolving manganese complex of green algae and higher plants investigated by X-ray absorption linear dichroism spectroscopy on oriented photosystem II membrane particles. *Biochemistry 37*, 7340–7350.

(98) Yachandra, V. K., Sauer, K., and Klein, M. P. (1996) Manganese cluster in photosynthesis: Where plants oxidize water to dioxygen. *Chem. Rev. 96*, 2927–2950.

(99) Law, N. A., Kampf, J. W., and Pecoraro, V. L. (2000) A magneto-structural correlation between the Heisenberg constant, J, and the Mn-O-Mn angle in $[Mn_{IV}(\mu\text{-O})]_2$ dimers. *Inorg. Chim. Acta 297*, 252–264.

(100) Randall, D. W., Sturgeon, B. E., Ball, J. A., Lorigan, G. A., Chan, M. K., Klein, M. P., Armstrong, W. H., and Britt, R. D. (1995) ^{55}Mn ESE-ENDOR of a mixed valence Mn(III)Mn(IV) complex: Comparison with the Mn cluster of the photosynthetic oxygen-evolving complex. *J. Am. Chem. Soc. 117*, 11780–11789.

(101) Randall, D. W., Chan, M. K., Armstrong, W. H., and Britt, R. D. (1998) Pulsed ^{1}H and ^{55}Mn ENDOR studies of dinuclear Mn(III)Mn(IV) model complexes. *Mol. Phys. 95*, 1283–1294.

(102) Manchanda, R., Brudvig, G. W., and Crabtree, R. H. (1995) High-valent oxomanganese clusters: Structural and mechanistic work relevant to the oxygen-evolving center in photosystem II. *Coord. Chem. Rev. 144*, 1–38.

(103) Liang, W., Latimer, M. J., Dau, H., Roelofs, T. A., Yachandra, V. K., Sauer, K., and Klein, M. P. (1994) Correlation between structure and magnetic spin state of the manganese cluster in the oxygen-evolving complex of photosystem II in the S_2 state: Determination by X-ray absorption spectroscopy. *Biochemistry 33*, 4923–4932.

(104) Peloquin, J. M., Campbell, K. A., Randall, D. W., Evanchik, M. A., Pecoraro, V. L., Armstrong, W. H., and Britt, R. D. (2000) ^{55}Mn-ENDOR of the S_2-state multiline EPR signal of photosystem II: Implications on the structure of the tetranuclear Mn cluster. *J. Am. Chem. Soc. 122*, 10926–10942.

(105) Wieghardt, K. (1989) The active sites in manganese-containing metalloproteins and inorganic model complexes. *Angew. Chem., Int. Ed. 28*, 1153–1172.

(106) Thorp, H. H., and Brudvig, G. W. (1991) The physical inorganic chemistry of manganese relevant to photosynthetic oxygen evolution. *New J. Chem. 15*, 479–490.